Article:
Wu, T. and Chen, B. (2016) Synthesis of Multiwalled Carbon Nanotube-Reinforced Polyborosiloxane Nanocomposites with Mechanically Adaptive and Self-Healing Capabilities for Flexible Conductors. ACS Applied Materials & Interfaces. ISSN: 1944-8244

https://doi.org/10.1021/acsami.6b06137

Synthesis of multi-walled carbon nanotube-reinforced polyborosiloxane nanocomposites with mechanically adaptive and self-healing capabilities for flexible conductors

Tongfei Wu and Biqiong Chen*

Department of Materials Science and Engineering, University of Sheffield, Mappin Street, Sheffield S1 3JD, UK.

ABSTRACT: Intrinsic self-healing polyborosiloxane (PBS) and its multi-walled carbon nanotube (MWCNT)-reinforced nanocomposites were synthesized from hydroxyl terminated poly(dimethylsiloxane) (PDMS) and boric acid at room temperature. The formation of Si-O-B moiety in PBS was confirmed by Fourier transform infrared spectroscopy. PBS and its MWCNT-reinforced nanocomposites were found possessing water or methanol activated mechanically adaptive behaviors; the compressive modulus decreased substantially when exposed to water or methanol vapor and recovered their high value after the stimulus was removed. The compressive modulus was reduced by 76%, 86%, 90% and 83% for neat PBS and its nanocomposites containing 3.0 wt.%, 6.2 wt.% and 13.3 wt.% MWCNTs, respectively, in water vapor, and the modulus reduction activated by methanol vapor was greater than by water vapor. MWCNTs at higher contents acted as a continuous electrical channel in PBS offering electrical conductivity, which was up to 1.21 S/cm for the nanocomposite containing 13.3 wt.% MWCNTs. The MWCNT-reinforced PBS nanocomposites also showed excellent mechanically and electrically self-healing properties, moldability and adhesion to PDMS elastomer substrate. These properties enabled a straightforward fabrication of self-repairing MWCNT/PBS electronic circuits on PDMS elastomer substrates.

Keywords: *adaptive properties, conducting nanocomposites, multi-walled carbon nanotubes, polyborosiloxane, self-healing*

INTRODUCTION

Self-healing chemistry, inspired by the self-healing capacity of organisms after injuries, is receiving growing research interests over the last decade.[1-6] Materials decorated with self-healing feature could boost the lifetime of products and build new potentials in various areas.[7] Self-healing conductors are currently attracting a significant number of studies,[8-16] particularly for advanced electronic applications, including chemical sensors,[17] thermal sensors,[18] supercapacitors,[19-21] lithium-ion batteries,[2] and electronic skin.[7, 22] Similarly, flexible conductors play an important role in the emerging fields, such as prosthetics, soft robotics, stretchable displays and human–machine interfaces.[23-25] The flexibility of existing flexible electrodes is mainly determined by the electrically conductive materials and their assembly on elastomeric substrates.[26] During repeated distortions, particularly under lager deformations, some irreversibly mechanical damages are inevitable in conventional conductive materials because of their high rigidity. Therefore, the capability of self-healing conductors to reconstruct the electrical conductivity with no external help could be a significant advancement for fabricating novel electronic devices.[11,27] The incorporation of conducting fillers into a self-healing matrix (e.g. intrinsic self-healing gels[26,28-31] and polymers[7, 22,32]) to form self-healing composites is an attractive strategy to achieve conductors which intrinsically self-heal at ambient temperature. These composites have an advantage that their self-healing function can serve multiple times, promising repeatable recovery of mechanical and electrical properties.[33] The reversible bonds in the matrix, which can be either covalent or non-covalent, underpin the self-healing mechanism,[34] allowing repair at the molecular level to restore the properties of original materials. Most self-healing processes involve an external energy source (*e.g.* heat or light) for the association or dissociation of reversible bonds.[33] To achieve the intrinsic, room-temperature self-healing capability, a number of dynamic reversible bonds, of which the association or dissociation can occur spontaneously at ambient conditions, have been widely studied, including hydrogen bonding,[35-37] metal-ligand interaction,[38] π-π stacking,[39] molecular interdiffusion,[40] and boron/oxygen dative bond.[41]

Polyborosiloxane (PBS) is an intrinsic, room-temperature self-healing supramolecular material based on the boron/oxygen dative bond.[7] The boron atom in Si-O-B moiety of PBS could form boron/oxygen dative bonds with oxygen atom in adjacent PBS chains, resulting in cross-linked networks (Figure 1a). Because of the dynamic nature of boron/oxygen dative bond, PBS behaves like an

elastic solid for high Deborah numbers under a rapid strain variation, yet like a viscous fluid over longer testing time scales.[42] This fascinating viscoelastic property has attracted considerable industrial and academic interests over the past decade, such as modelling martials for education[43] and insulated materials for LED encapsulation.[44] Lately, D'Elia and co-workers[7] embedded reduced graphene oxide scaffolds in PBS and achieved multifunctional self-healing composites with a conductivity up to 0.9 S/cm and pressure and flexion sensing capabilities. PBS is synthesized through the modification of poly(dimethylsiloxane) (PDMS) (in which the glass transition temperature Tg < -120 °C[45]) using boric acid.[46] The conventional recipes are achieved at elevated temperatures (> 150 °C), where boric acid facilitates the chain cleavage by grafting to the ends of the cut PDMS chains.[43] However, besides the desired Si-O-B moiety, self-polymerization of boric acid also occurs at elevated temperatures, leading to the formation of by-product boroxane (B-O-B) moiety.[46] To obtain purified PBSs, a refinement step to remove the B-O-B moiety (i.e. hydrolysis of the B-O-B bonds and subsequent removal of the released boric acid) is crucial.[43]

Herein, we provided a facile method to synthesize a self-healing PBS at room temperature, as well as its multi-walled carbon nanotube (MWCNT)-reinforced nanocomposites. The formation of Si-O-B moiety and the absence of B-O-B moiety were identified by using Fourier transform infrared (FTIR) spectroscopy. MWCNTs acted as the conducting channel in PBS raising the electrical conductivity up to 1.21 S/cm for the nanocomposite containing 13.3 wt.% MWCNTs. The MWCNT/PBS nanocomposites also exhibited unique features, including water or methanol activated adaptive properties, mechanically and electrically self-healing properties, versatile moldability, and excellent adhesion to conventional PDMS elastomer substrate. These features enabled a readily fabrication of flexible electronic circuits on PDMS elastomer substrates, which could restore their conductivities after damages.

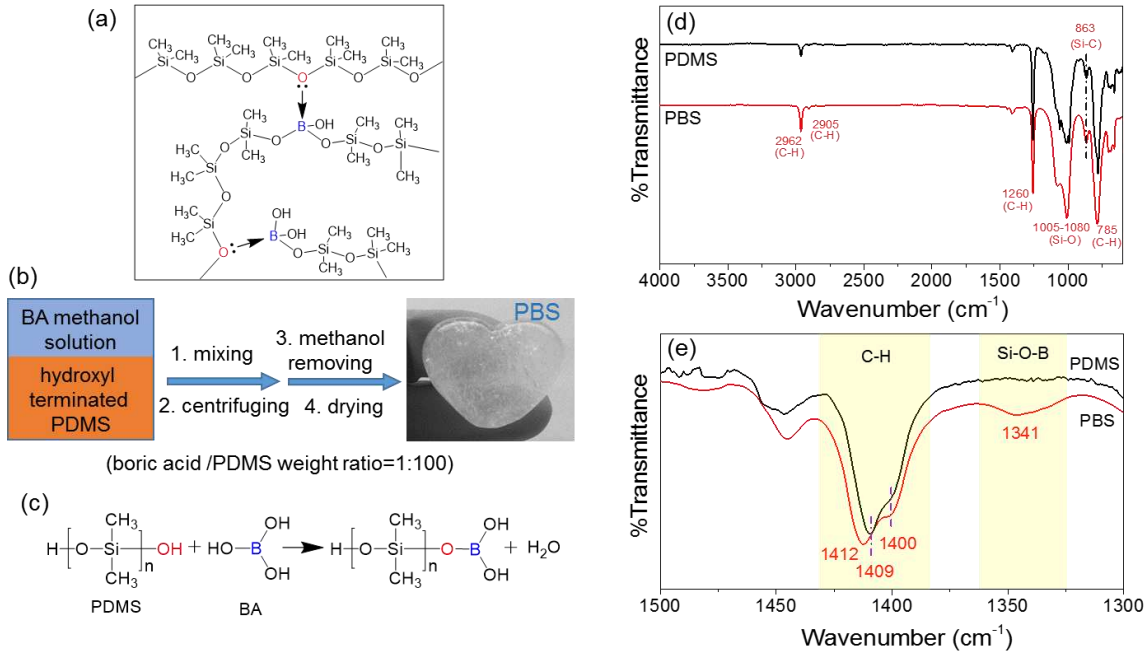

Figure 1. a) Schematic PBS network cross-linked by boron/oxygen dative bonds and b) the pathway to the synthesis of polyborosiloxane (PBS) through modifying hydroxyl terminated polydimethylsiloxane (PDMS) using boric acid (BA) at ambient temperature. c) Schematic condensation of boric acid with one silanol end of PDMS. d,e) FTIR spectra of hydroxyl terminated PDMS and PBS.

RESULTS AND DISCUSSION

Synthesis of Self-healing PBS. Self-healing PBS was prepared from hydroxyl terminated PDMS and boric acid at ambient temperature (20 °C), as shown in Figure 1b. Firstly, PDMS was mixed with a boric acid methanol solution, expecting the condensation of boric acid with the silanol ends of PDMS (Figure 1c). Because of the poor compatibility between methanol and PDMS, two liquid phases were found existing throughout the mixing process under continuously stirring. After centrifugation, methanol locating at the top layer could be easily removed (Figure S1 in Supporting Information) and the modified PDMS (*i.e.* PBS) remained the capability to flow. However, this product became non-tacky, viscoelastic and deformable after methanol evaporation, which appeared completely different from the original PDMS liquid. FTIR spectra of PDMS and PBS are compared in Figure 1(d,e),

confirming the formation of Si-O-B moiety by the presence of the characteristic peak of Si-O-B at 1341 cm^{-1} (Figure 1e).[43] It is noted that there is no peak at 1380 cm^{-1} characteristic for B-O-B, indicating the absence of the B-O-B moiety. This suggests that the boric acid has only reacted with the silanol ends of PDMS chains transforming PDMS into PBS and avoiding the formation of the B-O-B moiety from the excess and free boric acid. The peaks at 785 cm^{-1} (C-H rocking), 1260 cm^{-1} (C-H symmetric bending), 1409 cm^{-1} (C-H asymmetric bending), 2906 cm^{-1} (C-H symmetric stretching), and 2962 cm^{-1} (C-H asymmetric stretching) are attributed to the IR absorption of $Si-CH_3$ moiety, while the peak at 863 cm^{-1} for Si-C (stretching) and the band at 1005-1080 cm^{-1} (Si-O stretching) are for Si-O-Si/Si-O-H moiety.[47-49]

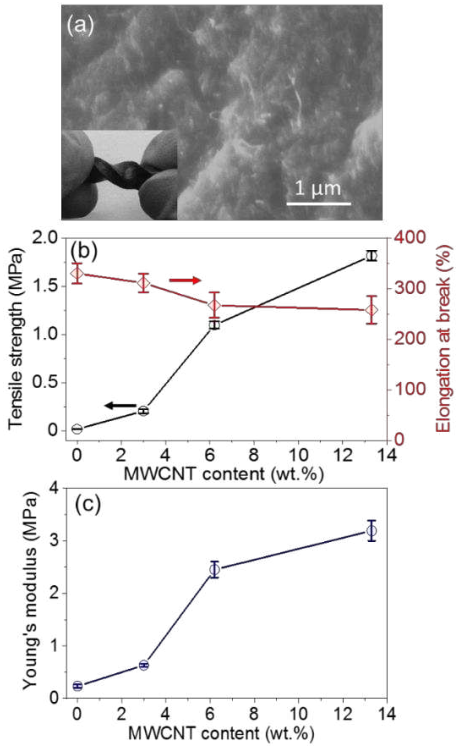

Figure 2. a) A cross-sectional SEM image of MWCNT/PBS 13.3% (Inset: A photograph of the nanocomposite, showing excellent flexibility). Mechanical characterization of MWCNT/PBS nanocomposites with various MWCNT contents: (b) tensile strength and elongation at break, and (c) Young's modulus.

Mechanical Properties of MWCNT/PBS Nanocomposites. To investigate the influence of MWCNTs on the electrical and mechanical properties, as well as the self-healing performance of PBS, we proceeded to prepare three MWCNT/PBS nanocomposites with different contents of MWCNTs at 3.0 wt.%, 6.2 wt.% and 13.3 wt.%. These three contents were selected to achieve a good balance of the mechanical properties and the self-healing efficiency, as it was expected that a higher content of MWCNTs could improve the tensile strength, Young's modulus and electrical conductivity of the polymer matrix, but decrease the self-healing ability. MWCNT/PBS nanocomposites were prepared by shear mixing MWCNTs with the BA-modified PDMS in its methanol dispersion. This was followed by the same centrifugation and drying procedure to remove solvent as for the preparation of neat PBS. As expected, the cross-sectional scanning electron microscopic (SEM) images display that the amount of MWCNTs at the fracture surface increases with increasing content of MWCNTs (Figure S2). The high resolution SEM image of the 13.3 wt.% sample (MWCNT/PBS 13.3%) in Figure 2a shows a relatively uniform dispersion of MWCNTs in the polymer matrix.

The reinforcement of MWCNTs on mechanical properties of PBS is investigated by tensile testing, and the results are summarized in Figure 2(b,c). The tensile strength, elongation at break, and Young's modulus are 27.1 kPa, 327%, and 0.235 MPa for neat PBS, respectively. The tensile strength increases with MWCNT content. The incorporation of MWCNTs raises the tensile strength of PBS up to 1.81 MPa for MWCNT/PBS 13.3%, demonstrating efficient stress transfer in the nanocomposite. The elongation at break of MWCNT/PBS nanocomposites decreases slightly with increased content of MWCNTs, due to the confinement effect of nanofillers on the mobility of polymer chains.[50] However, it remains at a relatively high level for all MWCNT/PBS nanocomposites; for MWCNT/PBS 13.3%, the elongation at break is 259%. Young's modulus of MWCNT/PBS nanocomposites increases significantly with the content of MWCNTs. The improvements are 1.7, 9.1 and 13 times for MWCNT/PBS 3.0%, MWCNT/PBS 6.2% and MWCNT/PBS 13.3%, respectively, in comparison with neat PBS. These improvements are attributable to the high mechanical properties of MWCNTs and a good dispersion of MWCNTs in the matrix, as well as the high aspect ratio of MWCNTs which may lead to interlaced structure of MWCNTs, especially at a high MWCNT content, to further reinforce the material. It is clear from the above results that increasing the MWCNT content strengthens the material by increasing the Young's modulus and the maximum tensile stress that the nanocomposite can withstand. It is also noted that the MWCNT/PBS nanocomposites can be molded into bulk parts or films by compression due to the unique viscoelastic property of PBS and that the nanocomposites can withstand a large flexion (Figure 2a Inset).

Stimulus-induced Adaptive Properties of MWCNT/PBS Nanocomposites. Inspired by the consolidation process of PBS and the nature of boron/oxygen dative bond, a molecule (e.g. water or methanol) that can provide a pair of electrons to the boron atom is expected to be able to competitively break the cross-linking bonds in PBS (Figure 3a Inset). Therefore, the macroscopic mechanical properties of PBS-based materials can be reversibly adjusted through controlling the equilibrium of this

competitive reaction. To inspect this prediction, the influences of water and methanol on PBS and its MWCNT-reinforced nanocomposites are investigated via compressive testing (Figure S3) and the changes in compressive modulus are summarized in Figure 3(a,b). All samples exhibit stimulus-responsive mechanically adaptive properties. PBS even became liquid after kept in methanol saturated vapor for 24 h (Figure S4a) and so the compression test did not proceed. In comparison, MWCNT/PBS nanocomposites remained intact due to the presence of MWCNTs, but were significantly softened by water vapor or methanol vapor (Figure S4b). Consequently, the compressive moduli of the nanocomposites decrease substantially after kept in the saturated vapor of water or methanol for 24 h. These reductions confirm the earlier postulation that water or methanol vapor can break the cross-linking boron/oxygen bonds in PBS, leading to a significant reduction in the modulus. The modulus reduction activated by methanol vapor is greater than water vapor. For instance, with saturated water vapor as stimulus, compressive moduli were reduced by 76%, 86%, 90% and 83% for PBS, MWCNT/PBS 3.0%, MWCNT/PBS 6.2% and MWCNT/PBS 13.3%, respectively, in comparison to the values of original samples. With methanol saturated vapor as stimulus, compressive moduli were reduced by 96%, 94% and 93% for MWCNT/PBS 3.0%, MWCNT/PBS 6.2% and MWCNT/PBS 13.3%, respectively. After the vapor-saturated nanocomposites were kept in ambient conditions for 8 h, they all recovered their original modulus values, demonstrating reversibility (Figure 3(a,b)). It is noted that the recovered compressive modulus of MWCNT/PBS 13.3% was slightly larger than the original one with methanol saturated vapor as stimulus. This might be caused by the slight changes in recovered chemical cross-linking structures, as well as the rearrangement of MWCNTs after being softened.

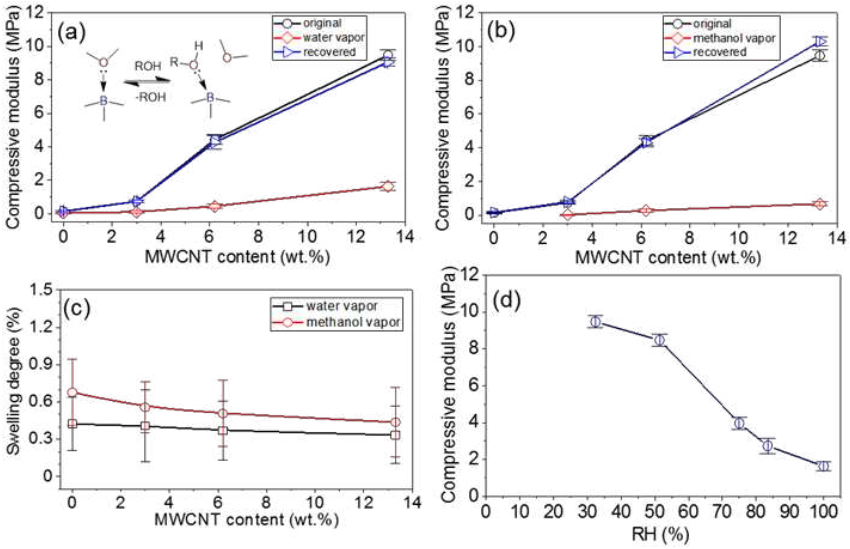

Figure 3. Mechanically adaptive properties of MWCNT/PBS nanocomposites: the changes in compressive modulus activated by the saturated vapors of (a) water and (b) methanol. Inset of a: The proposed mechanism of chemical-activated mechanically adaptive property of PBS (ROH = methanol or water). c) Swelling degree of MWCNT/PBS nanocomposites as a function of MWCNT content. d) Compressive modulus of MWCNT/PBS 13.3% as a function of relative humidity (RH).

We also measured the swelling degrees (the weight increments) of all the samples after kept in water or methanol saturated vapor for 24 h, as shown in Figure 3c. It can be seen that the swelling degrees in both methanol and water saturated vapors are quite low (< 0.8%), further confirming the softening effect was induced by the breaking of boron/oxygen dative bonds rather than swelling. We also studied the compressive modulus of MWCNT/PBS 13.3% under varying relative humidity (RH) as shown in Figure 3d. The compressive modulus decreased with increasing RH. The reduction is from 82% for 32% RH to 100% RH. This suggests that increasing the water vapor pressure in the environment can lead to a higher degree of modulus reduction; a high water vapor pressure makes the reaction equilibrium shift towards right side in Figure 3a Inset, resulting in the break of the cross-linking bonds and consequently the reduced modulus. By comparing the FTIR spectra of the PBS samples after vapor swelling with that of the original PBS (Figure S5), it can be seen that the peak of Si-O-B moiety significantly diminishes after swelling in methanol vapor, while there are almost no changes for the peak after swelling in water vapor. This suggests that methanol molecules can not only affect the formation of the boron/oxygen dative bond in PBS, but also break O-B bond in Si-O-B moiety, resulting in the high efficiency of softening. This might be caused by its high vapor pressure (660 kPa for methanol at 20 °C versus 2.3 kPa for water),[51] and presumably its high reactivity as well.

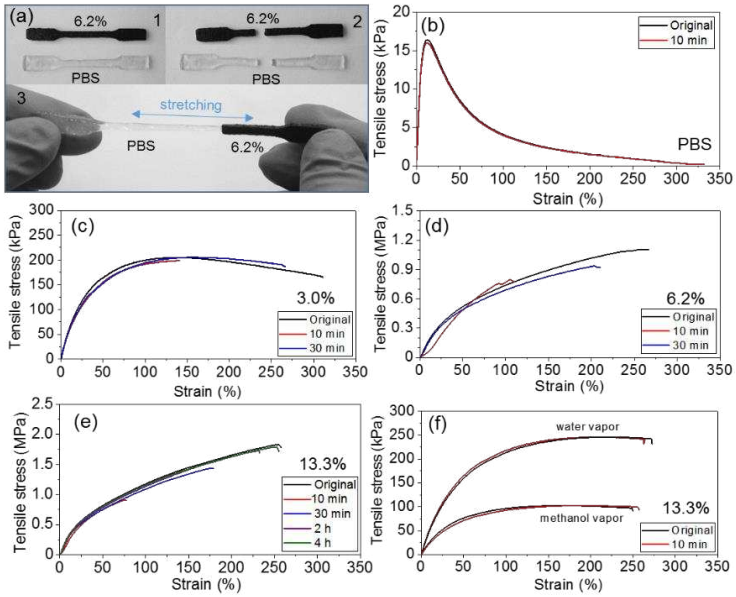

Figure 4. a) Demonstration of the self-healing properties of PBS and MWCNT/PBS 6.2%: 1) undamaged samples; 2) completely severed samples; 3) mechanically self-healed sample. Representative tensile stress-strain curves of original and healed samples for different healing durations under ambient conditions: b) PBS, c) MWCNT/PBS 3.0%, d) MWCNT/PBS 6.2%, and e) MWCNT/PBS 13.3%. f) Representative tensile stress-strain curves of the original and the healed MWCNT/PBS 13.3%, both saturated in water or methanol vapor. For the self-healing test, the sample was cut into two pieces with a scalpel and then the two broken pieces were pushed into contact by hand under a low pressure (~ 1 kPa) for ~1 s, followed by being allowed to heal at free-stress state for a period of time.

Table 1. Self-healing performance of PBS and MWCNT/PBS nanocomposites.[a]

Sample	Self-healing efficiency				
	Mechanical				Conductive
	10 min	30 min	2 h	4 h	10 sec
PBS	99.6±0.4%	--	--	--	--
MWCNT/PBS 3.0%	39.5±3.3%	86.3±2.8%	--	--	98.1±0.8%
MWCNT/PBS 6.2%	26.2±2.7%	66.0±3.1%	--	--	98.7±0.7%
MWCNT/PBS 13.3%	13.9±1.5% , 96.7±2.1% (w)[b], 98.4±0.9% (m)[b]	52.5±2.9%	84.4±2.2%	96.7±1.3%	97.9±0.8%

[a] Unless otherwise noted, the values presented in this table represent the results of the samples healed under ambient conditions. [b] w = healed with water vapor, m = healed with methanol vapor.

Self-healing Properties of MWCNT/PBS Nanocomposites. A key feature of PBS is its intrinsic, room-temperature mechanically self-healing property. It means, when PBS suffers cracks or fractures, simply bringing the broken pieces together will lead to spontaneous healing. Figure 4a demonstrates the mechanically self-healing behavior of PBS and its MWCNT-reinforced nanocomposites (more demonstrations in Figure S6). According to the previous work,[22] the mechanical healing efficiency can be calculated as the ratio of the restored toughness to the original toughness, where toughness is determined as the area under the stress-strain curve. Figure 4b-e exhibits the typical tensile stress–strain curves of samples with different healing durations, and the results are summarized in Table 1. The self-healing test was repeated three times for each self-healing condition. The toughness of neat PBS can fully (99.6%) recover after 10 min of contact. For MWCNT/PBS nanocomposites, the self-healing capability decreased with increasing MWCNT content, for example, from 39.5% for MWCNT/PBS 3.0% to 13.9% for MWCNT/PBS 13.3%. It can be attributed to the fact that the presence of MWCNTs at the fracture surface blocks the contact of PBS chains, forming remnant defects. On the other hand, MWCNTs could also form a rigid network, hindering the flow of PBS from contact by confining PBS chains. The healing efficiency could be further

improved by extending the healing duration. For instance, the healing efficiency increased from 39.5% after 10 min of contact to 86.3% after 30 min of contact for MWCNT/PBS 3.0%. In the case of MWCNT/PBS 13.3%, the healing efficiency reached 96.7% for 4 h of contact. Furthermore, the self-healing performance can be improved by placing the damaged sample in an environment that is rich of water or methanol vapor, because the vapor will soften the matrix through breaking the cross-linkage in PBS and improve the mobility of PBS chains for healing (Figure 4f). For instance, the healing efficiency of MWCNT/PBS 13.3% reached 96.7% and 98.4% after 10 min of contact in water and methanol vapors, respectively (Table 1).

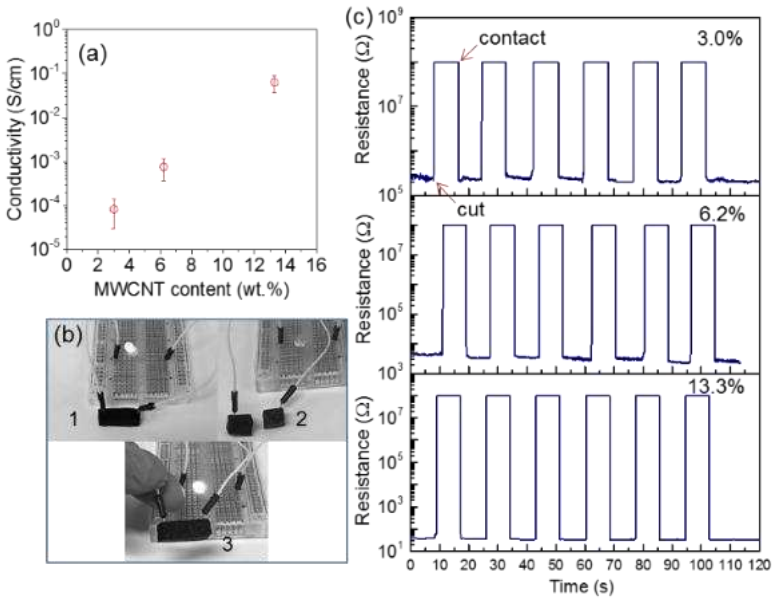

Figure 5. a) Electrical conductivities of MWCNT/PBS nanocomposites. b) Demonstration of the electrical healing process for MWCNT/PBS 13.3% in an LED-integrated circuit: 1. original MWCNT/PBS (LED on); 2. completely fractured MWCNT/PBS (Namely, open circuit, LED off); and 3. electrically self-healed MWCNT/PBS. c) The resistance changes of MWCNT/PBS nanocomposites as a function of time during the repeated electrical healing process at ambient temperature. For the self-healing test, the sample was cut into two pieces with a scalpel and then the two broken pieces were pushed into contact by hand under a low pressure (~ 1 kPa) for ~1 s, followed by being allowed to heal at free-stress state for 10 s.

The MWCNT network provides a continuous conducting channel in MWCNT/PBS nanocomposites. The electrical conductivity is 3.34×10^{-4} S/cm, 2.91×10^{-2} S/cm and 1.21 S/cm as measured for MWCNT/PBS 3.0%, 6.2% and 13.3%, respectively (Figure 5a). It is noted that there are no significant changes in the electrical conductivity after water or methanol absorption, indicating the low swelling degree does not influence the MWCNT network in the matrix. Figure 5b demonstrates the self-repairing behavior of an intrinsic, room-temperature self-healing nanocomposite in an electronic circuit. The change in resistance during the repeated self-healing processes is shown in Figure 5c. It can be seen that the resistance immediately dropped to nearly its original value, once the two fracture surfaces were brought together. The conductive healing efficiency is determined as the ratio of the restored conductivity to the original conductivity. The conductive healing efficiency is calculated as high as 98% for all MWCNT/PBS nanocomposites (Table 1).

Demonstration of MWCNT/PBS Nanocomposites as Flexible Conductors on PDMS. PBS is expected to form strong bonding with PDMS elastomer substrate through boron/oxygen dative bond. Therefore, the conducting MWCNT/PBS nanocomposites can adhere to PDMS elastomers themselves, which is very attractive in fabricating flexible conductors. Figure 6a shows the peel strength between PBS and PDMS elastomer substrate. It was found that the fracture happened in the PBS layer, instead of the interface between PBS and PDMS elastomer substrate (Figure S7a,b), indicating the bonding strength between PBS and PDMS was higher than the strength of PBS. The incorporation of MWCNTs significantly improved the strength of PBS. Yet, failure again occurred in the nanocomposite layers instead of the interface and the peel strength was much higher than that with the pristine PBS. These results confirm a strong bonding between PBS-based materials and PDMS substrate, facilitating facile fabrication of high-performance flexible conductors. The change in resistance of MWCNT/PBS nanocomposites on PDMS substrate as a function of flexion angle is plotted in Figure 6b (setup shown in Figure S7c). The MWCNT/PBS nanocomposites show excellent electrical stability during the bending tests in which the resistances remain almost constant under different flexion angles between 0° and

90° for all samples. The self-healing property is another key feature when using MWCNT/PBS nanocomposites as the conductor. Figure 6c exhibits the self-repairing ability and flexibility of a circuit with MWCNT/PBS 13.3% as the conductor. The LED had negligible degradation in light intensity after bending and folding motions.

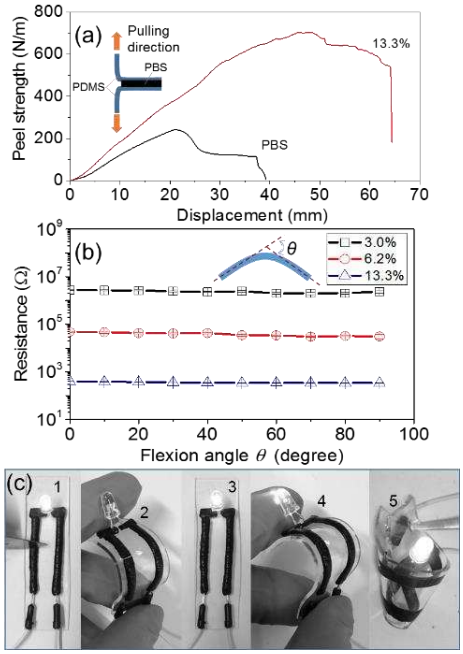

Figure 6. Electrical properties of MWCNT/PBS nanocomposites on PDMS substrate under ambient conditions. a) Peel strength–displacement curves for PBS and MWCNT/PBS 13.3% (Inset: a schematic for T-peel testing). b) Resistance of MWCNT/PBS nanocomposites as a function of flexion angle θ (Inset: definition of flexion angle θ). c) Demonstration of the healing process and flexibility of a circuit with an LED in series with MWCNT/PBS 13.3% as a self-healing conductor: 1. undamaged MWCNT/PBS; 2. completely severed MWCNT/PBS (LED off); 3. the restoration of the conductivity of MWCNT/PBS in the flattened circuit; 4. mechanically self-healed MWCNT/PBS after 24 h; 5. folded circuit.

CONCLUSIONS

In summary, we described a facile method to synthesize intrinsic self-healing PBS from hydroxyl terminated PDMS and boric acid at ambient temperature, as well as its MWCNT-reinforced nanocomposites. PBS and its MWCNT-reinforced nanocomposites exhibited water or methanol activated mechanically adaptive properties. The compressive modulus largely reduced when exposed to water or methanol vapor and recovered its high value after the stimulus was removed. For instance, the compressive modulus of the nanocomposite containing 6.2 wt.% MWCNTs was reduced by up to 90% in saturated water vapor, and the modulus reduction degree increased with increasing relative humidity. MWCNTs formed a network and acted as a continuous electrical channel in PBS rendering electrical conductivity, which were 2.91 × 10^{-2} S/cm and 1.21 S/cm for the nanocomposite containing 6.2 wt.% and 13.3 wt.% MWCNTs, respectively. MWCNT-reinforced PBS nanocomposites also had other capabilities, such as repetitive rapid mechanically and electrically self-healing ability (53% mechanical healing efficiency with a 30 min recovery duration and 98% conductive healing efficiency with a 10 s recovery duration for the 13.3% MWCNT/PBS nanocomposite at ambient conditions, or 97% mechanical healing efficiency with a 10 min recovery duration with water vapor), being moldable into bulk parts or films, as well as excellent adhesion to PDMS elastomer substrate. These attractive features allowed for a facile manufacture of flexible, self-repairable electronic circuits on PDMS elastomer substrate.

EXPERIMENTAL SECTION

Materials. Polydimethylsiloxane (PDMS) (hydroxyl terminated, with a kinematic viscosity of 1.8~2.2×10^{-3} m^2/s), boric acid, multi-walled carbon nanotubes (MWCNTs, outer diameter: 10-15 nm, inner diameter: 2-6 nm and length: 0.1-10 μm), magnesium chloride hexahydrate ($MgCl_2{\cdot}6H_2O$), sodium chloride (NaCl), potassium chloride (KCl) and magnesium nitrate hexahydrate ($Mg(NO_3)_2{\cdot}6H_2O$) were purchased from Sigma-Aldrich and used as received.

Synthesis of polyborosiloxane (PBS). 20 g PDMS was added into 15 ml boric acid methanol solution (0.0133 g/ml) and continuously stirred for 1 h. The PDMS/boric acid weight ratio was 100:1. The mixture was centrifuged at 6,000 rpm for 5 min. After removing the top layer (i.e. methanol) by using a pipette, the product was poured into a petri dish and kept in a fume cupboard to evaporate most methanol. The typical period of time for the product to become non-tacky PBS was found as 2 h. Then the product was kept in vacuum at room temperature for 12 h to remove residual methanol.

Synthesis of MWCNT/PBS nanocomposites. MWCNT/PBS nanocomposites were prepared by mechanically mixing. 20 g PDMS was added into 15 ml boric acid methanol solution (13.3 mg/ml) and continuously stirred for 1 h. Then a desired amount of MWCNTs was added. The mixture was stirred at 10,000 rpm for 15 min using a Silverson shear mixer (model L5M-A), followed by centrifugation to remove methanol. The product was placed in a petri dish and kept in a fume cupboard for 2 h until the nanocomposite became non-tacky and in vacuum for 12 h to remove residual methanol. The nanocomposites containing 3.0 wt.%, 6.2 wt.%, and 13.3 wt.% MWCNTs were prepared.

Characterization. Attenuated total reflectance-Fourier transform infrared (ATR-FTIR) spectroscopy

was performed using a Frontier Optica spectrophotometer (PerkinElmer). The wavenumber region was between 4000 to 600 cm^{-1} and the resolution was 1 cm^{-1}. The microstructure of MWCNT/PBS nanocomposites was investigated by using scanning electron microscopy (Inspect F, FEI) at an acceleration voltage of 10 keV. The electrical properties of the sample were measured in two-point using an Agilent 34401A multimeter (Keysight Technologies Inc.). For the conductivity test, a cylindrical sample (Φ10 × 10 mm) was used. Tensile, compression and T-peel tests were carried out using a Lloyd universal testing machine (Ametek Inc.) with a 10 N load cell and 100 mm min–1 for the testing speed. Samples for the tensile test were punched from a sheet sample with a thickness of ~ 1.5 mm into a dumbbell shape (ISO 527-2-1A type). Five specimens were tested for each measurement. For compression test, a cylinder sample (Φ10 × 5 mm) was used. To investigate the influence of humidity on the mechanical properties of the 13.3 wt.% MWCNT/PBS nanocomposite, the cylindrical sample (Φ10 × 5 mm) was kept under constant relative humidity (RH) for 24 h before each compression test. Saturated solutions were employed to control the RH in an enclosed environment: KCl for 83% RH, NaCl for 75% RH, Mg $(NO_3)_2$ for 51% RH and $MgCl_2$ for 32% RH at 20 °C.[52] For T-peel testing, PDMS elastomer sheets were prepared from Sylgard 184 Kit (Dow Corning) by curing at 60 °C for 2 h. The PBS-based samples with a 0.5 mm thickness were placed between two PDMS elastomer strips (2 × 20 ×50 mm^3 cut from PDMS elastomer sheets) by applying a pressure (~ 1 MPa). The joint area was 20 × 15 mm^2. The sandwich structure was kept in ambient conditions for 12 h before testing. To measure swelling degrees of PBS and MWCNT/PBS nanocomposites in water and methanol saturated vapors, equation (1) was used.

$$\text{Swelling degree} = (W_2 - W_1)/W_1 \times 100\% \quad (1)$$

where W_1 is the original weight of samples and W_2 is the weight of samples after kept in water and methanol saturated vapors for 24 h.

ASSOCIATED CONTENT

Supporting Information.

This material is available free of charge via the Internet at http://pubs.acs.org.

Photographs of preparation of PBS, PBS and MWCNT/PBS with adaptive and self-healing properties, and setups for T-peel and flexion tests. Cross-section SEM images of MWCNT/PBS. Typical compressive stress-strain curves of adaptive behaviours of PBS and MWCNT/PBS.

AUTHOR INFORMATION

Corresponding Author

* E-mail: biqiong.chen@sheffield.ac.uk.

Notes

The authors declare no competing financial interest.

ACKNOWLEDGEMENTS

This project is supported by the European Commission's Horizon 2020 research and innovation programme under the Marie Skłodowska-Curie grant agreement No 656467.

REFERENCES

(1) de Espinosa, L. M.; Fiore, G. L.; Weder, C.; Johan Foster, E.; Simon, Y. C. Healable Supramolecular Polymer Solids. *Prog. Polym. Sci.* **2015,** *49–50*, 60-78.

(2) Wang, C.; Wu, H.; Chen, Z.; McDowell, M. T.; Cui, Y.; Bao, Z. Self-Healing Chemistry Enables the Stable Operation of Silicon Microparticle Anodes for High-Energy Lithium-Ion Batteries. *Nat. Chem.* **2013,** *5*, 1042-1048.

(3) Hillewaere, X. K. D.; Du Prez, F. E. Fifteen Chemistries for Autonomous External Self-Healing Polymers and Composites. *Prog. Polym. Sci.* **2015,** *49–50*, 121-153.

(4) Yin, X.; Liu, Z.; Wang, D.; Pei, X.; Yu, B.; Zhou, F. Bioinspired Self-Healing Organic Materials: Chemical Mechanisms and Fabrications. *J. Bionic. Eng.* **2015,** *12*, 1-16.

(5) Wong, T. S.; Kang, S. H.; Tang, S. K. Y.; Smythe, E. J.; Hatton, B. D.; Grinthal, A.; Aizenberg, J. Bioinspired Self-Repairing Slippery Surfaces with Pressure-Stable Omniphobicity. *Nature* **2011,** *477*, 443-447.

(6) Li, Y.; Li, L.; Sun, J. Bioinspired Self-Healing Superhydrophobic Coatings. *Angew. Chem., Int. Ed.* **2010,** *49*, 6129-6133.

(7) D'Elia, E.; Barg, S.; Ni, N.; Rocha, V. G.; Saiz, E. Self-Healing Graphene-Based Composites with Sensing Capabilities. *Adv. Mater.* **2015,** *27*, 4788-4794.

(8) Blaiszik, B. J.; Kramer, S. L. B.; Grady, M. E.; McIlroy, D. A.; Moore, J. S.; Sottos, N. R.; White, S. R. Autonomic Restoration of Electrical Conductivity. *Adv. Mater.* **2012,** *24*, 398-401.

(9) Williams, K. A.; Boydston, A. J.; Bielawski, C. W. Towards Electrically Conductive, Self-Healing Materials. *J. R. Soc., Interface* **2007,** *4*, 359-362.

(10) Li, Y.; Chen, S.; Wu, M.; Sun, J. Polyelectrolyte Multilayers Impart Healability to Highly Electrically Conductive Films. *Adv. Mater.* **2012,** *24*, 4578-4582.

(11) Sun, H.; You, X.; Jiang, Y.; Guan, G.; Fang, X.; Deng, J.; Chen, P.; Luo, Y.; Peng, H. Self-Healable Electrically Conducting Wires for Wearable Microelectronics. *Angew. Chem., Int. Ed.* **2014,** *53*, 9526-9531.

(12) Guo, K.; Zhang, D. L.; Zhang, X. M.; Zhang, J.; Ding, L. S.; Li, B. J.; Zhang, S. Conductive Elastomers with Autonomic Self-Healing Properties. *Angew. Chem., Int. Ed.* **2015,** *54*, 12127-12133.

(13) Palleau, E.; Reece, S.; Desai, S. C.; Smith, M. E.; Dickey, M. D. Self-Healing Stretchable Wires for Reconfigurable Circuit Wiring and 3D Microfluidics. *Adv. Mater.* **2013,** *25*, 1589-1592.

(14) Zhang, D. L.; Ju, X.; Li, L. H.; Kang, Y.; Gong, X. L.; Li, B. J.; Zhang, S. An Efficient Multiple Healing Conductive Composite via Host-Guest Inclusion. *Chem. Commun.* **2015,** *51*, 6377-6380.

(15) Diesendruck, C. E.; Sottos, N. R.; Moore, J. S.; White, S. R. Biomimetic Self-Healing. *Angew. Chem., Int. Ed.* **2015,** *54*, 10428-10447.

(16) O'Connor, T. F.; Rajan, K. M.; Printz, A. D.; Lipomi, D. J. Toward Organic Electronics with Properties Inspired by Biological Tissue. *J. Mater. Chem. B* **2015,** *3*, 4947-4952.

(17) Huang, W.; Besar, K.; Zhang, Y.; Yang, S.; Wiedman, G.; Liu, Y.; Guo, W.; Song, J.; Hemker, K.; Hristova, K.; Kymissis, I. J.; Katz, H. E. A High-Capacitance Salt-Free Dielectric for Self-Healable, Printable, and Flexible Organic Field Effect Transistors and Chemical Sensor. *Adv. Funct. Mater.* **2015,** *25*, 3745-3755.

(18) He, Y.; Liao, S.; Jia, H.; Cao, Y.; Wang, Z.; Wang, Y. A Self-Healing Electronic Sensor based on Thermal-Sensitive Fluids. *Adv. Mater.* **2015,** *27*, 4622-4627.

(19) Huang, Y.; Huang, Y.; Zhu, M.; Meng, W.; Pei, Z.; Liu, C.; Hu, H.; Zhi, C. Magnetic-Assisted, Self-Healable, Yarn-Based Supercapacitor. *ACS Nano* **2015,** *9*, 6242-6251.

(20) Huang, Y.; Zhong, M.; Huang, Y.; Zhu, M.; Pei, Z.; Wang, Z.; Xue, Q.; Xie, X.; Zhi, C. A Self-Healable and Highly Stretchable Supercapacitor Based on a Dual Crosslinked Polyelectrolyte. *Nat. Commun.* **2015,** *6*, 10310(1-8).

(21) Wang, H.; Zhu, B.; Jiang, W.; Yang, Y.; Leow, W. R.; Wang, H.; Chen, X. A Mechanically and Electrically Self-Healing Supercapacitor. *Adv. Mater.* **2014,** *26*, 3638-3643.

(22) Tee, B. C. K.; Wang, C.; Allen, R.; Bao, Z. An Electrically and Mechanically Self-Healing Composite with Pressure- and Flexion-Sensitive Properties for Electronic Skin Applications. *Nat. Nanotechnol.* **2012,** *7*, 825-832.

(23) Benight, S. J.; Wang, C.; Tok, J. B. H.; Bao, Z. Stretchable and Self-Healing Polymers and Devices for Electronic Skin. *Prog. Polym. Sci.* **2013,** *38*, 1961-1977.

(24) Kim, K.; Kim, J.; Hyun, B. G.; Ji, S.; Kim, S.; Kim, S.; An, B. W.; Park, J. Stretchable and Transparent Electrodes Based on In-Plane Structures. *Nanoscale* **2015**, 7, 14577-14594.

(25) Lee, M.; Lee, K.; Kim, S.; Lee, H.; Park, J.; Choi, K.; Kim, H.; Kim, D.; Lee, D.; Nam, S.; Park, J. High-Performance, Transparent, and Stretchable Electrodes Using Graphene–Metal Nanowire Hybrid Structures. *Nano Lett.* **2013**, 13, 2814-2821.

(26) Oh, J. Y.; Kim, S.; Baik, H. K.; Jeong, U. Conducting Polymer Dough for Deformable Electronics. *Adv. Mater.* **2016**, *28*, 4455-61.

(27) Odom, S. A.; Chayanupatkul, S.; Blaiszik, B. J.; Zhao, O.; Jackson, A. C.; Braun, P. V.; Sottos, N. R.; White, S. R.; Moore, J. S. A Self-Healing Conductive Ink. *Adv. Mater.* **2012,** *24*, 2578-2581.

(28) Peng, R.; Yu, Y.; Chen, S.; Yang, Y.; Tang, Y. Conductive Nanocomposite Hydrogels with Self-Healing Property. *RSC Adv.* **2014,** *4*, 35149-35155.

(29) Shi, Y.; Wang, M.; Ma, C.; Wang, Y.; Li, X.; Yu, G. A Conductive Self-Healing Hybrid Gel Enabled by Metal–Ligand Supramolecule and Nanostructured Conductive Polymer. *Nano Lett.* **2015**, 15, 6276-6281.

(30) Hur, J.; Im, K.; Kim, S. W.; Kim, J.; Chung, D.; Kim, T.; Jo, K. H.; Hahn, J. H.; Bao, Z.; Hwang, S.; Park, N. Polypyrrole/Agarose-Based Electronically Conductive and Reversibly Restorable Hydrogel. *ACS Nano* **2014**, 8, 10066-10076.

(31) Shi, Y.; Yu, G. Designing Hierarchically Nanostructured Conductive Polymer Gels for Electrochemical Energy Storage and Conversion. *Chem. Mater.* **2016**, 28, 2466-2477.

(32) Wu, T.; Chen, B. A Mechanically and Electrically Self-Healing Graphite Composite Dough for Stencil-Printable Stretchable Conductors. *J. Mater. Chem. C* **2016,** *4*, 4150-4154.

(33) Wojtecki, R. J.; Meador, M. A.; Rowan, S. J. Using the Dynamic Bond to Access Macroscopically Responsive Structurally Dynamic Polymers. *Nat. Mater.* **2011,** *10*, 14-27.

(34) Keller, M. W.; White, S. R.; Sottos, N. R. A Self-Healing Poly(Dimethyl Siloxane) Elastomer. *Adv. Funct. Mater.* **2007,** *17*, 2399-2404.

(35) Hentschel, J.; Kushner, A. M.; Ziller, J.; Guan, Z. Self-Healing Supramolecular Block Copolymers. *Angew. Chem., Int. Ed.* **2012,** *51*, 10561-10565.

(36) Chen, Y.; Kushner, A. M.; Williams, G. A.; Guan, Z. Multiphase Design of Autonomic Self-Healing Thermoplastic Elastomers. *Nat. Chem.* **2012,** *4*, 467-472.

(37) Cordier, P.; Tournilhac, F.; Soulie-Ziakovic, C.; Leibler, L. Self-Healing and Thermoreversible Rubber from Supramolecular Assembly. *Nature* **2008,** *451*, 977-980.

(38) Mozhdehi, D.; Ayala, S.; Cromwell, O. R.; Guan, Z. Self-Healing Multiphase Polymers via Dynamic Metal–Ligand Interactions. *J. Am. Chem. Soc.* **2014,** *136*, 16128-16131.

(39) Burattini, S.; Greenland, B. W.; Merino, D. H.; Weng, W.; Seppala, J.; Colquhoun, H. M.; Hayes, W.; Mackay, M. E.; Hamley, I. W.; Rowan, S. J. A Healable Supramolecular Polymer Blend Based on Aromatic π–π Stacking and Hydrogen-Bonding Interactions. *J. Am. Chem. Soc.* **2010,** *132*, 12051-12058.

(40) Rahman, M. A.; Sartore, L.; Bignotti, F.; Di Landro, L. Autonomic Self-Healing in Epoxidized Natural Rubber. *ACS Appl. Mater. Interfaces* **2013,** *5*, 1494-1502.

(41) Juhász, A.; Tasnádi, P.; Fábry, L. Impact Studies on the Mechanical Properties of Polyborosiloxane. *Phys. Educ.* **1984,** *19*, 302-304.

(42) Goertz, M. P.; Zhu, X. Y.; Houston, J. E. Temperature Dependent Relaxation of a "Solid–Liquid". *J. Polym. Sci., Part B: Polym. Phys.* **2009,** *47*, 1285-1290.

(43) Liu, Z.; Picken, S. J.; Besseling, N. A. M. Polyborosiloxanes (PBSs), Synthetic Kinetics, and Characterization. *Macromolecules* **2014,** *47*, 4531-4537.

(44) Katayama, H.; Akazawa, K. LED Device Comprising a Polyborosiloxane. EP 2014702 B1, 2009.

(45) Clarson, S. J.; Dodgson, K.; Semlyen, J. A. Studies of Cyclic and Linear Poly(Dimethylsiloxanes): 19. Glass Transition Temperatures and Crystallization Behaviour. *Polymer* **1985,** *26*, 930-934.

(46) Zinchenko, G. A.; Mileshkevich, V. P.; Kozlova, N. V. Investigation of the Synthesis and Hydrolytic Degradation of Polyborodimethylsiloxanes. *Polym. Sci. U.S.S.R.* **1981,** *23*, 1421-1429.

(47) Johnson, L. M.; Gao, L.; Shields IV, C. W.; Smith, M.; Efimenko, K.; Cushing, K.; Genzer, J.; López, G. P. Elastomeric Microparticles for Acoustic Mediated Bioseparations. *J. Nanobiotechnol.* **2013,** *11*, 1-8.

(48) Nour, M.; Berean, K.; Griffin, M. J.; Matthews, G. I.; Bhaskaran, M.; Sriram, S.; Kalantar-zadeh, K. Nanocomposite Carbon-PDMS Membranes for Gas Separation. *Sens. Actuators, B* **2012,** *161*, 982-988.

(49) Bae, S. C.; Lee, H.; Lin, Z.; Granick, S. Chemical Imaging in a Surface Forces Apparatus: Confocal Raman Spectroscopy of Confined Poly(Dimethylsiloxane). *Langmuir* **2005,** *21*, 5685-5688.

(50) Rittigstein, P.; Priestley, R. D.; Broadbelt, L. J.; Torkelson, J. M. Model Polymer Nanocomposites Provide an Understanding of Confinement Effects in Real Nanocomposites. *Nat. Mater.* **2007**, 6, 278-282.

(51) Dean, J. A. *Lange's Handbook of Chemistry*. 15th ed.; Mcgraw-Hill Inc.: London, 1999.

(52) Young, J. F. Humidity Control in the Laboratory using Salt Solutions—a Review. *J. Appl. Chem. (London, U.K.)* **1967,** *17*, 241-245.

Table of Contents